engineering proceedings

MDPI

Proceeding Paper

Mechanical Characterization of Triply Periodic Minimal Surface Structures Fabricated via SLA 3D Printing Using Tough Resin: Influence of Geometry on Performance †

Sofia Kavafaki * and Georgios Maliaris

Hephaestus Laboratory, School of Chemistry, Faculty of Sciences, Democritus University of Thrace, GR 65404 Kavala, Greece; gmaliari@chem.duth.gr

* Correspondence: skavafak@chem.duth.gr

† Presented at the 5th International Electronic Conference on Applied Sciences, 4–6 December 2024; Available online: https://sciforum.net/event/ASEC2024.

Abstract: Triply periodic minimal surfaces (TPMSs) structures are particularly suited for energy-absorbing, light-weight applications in fields such as medicine and engineering due to their ability to achieve maximum stress distribution with minimum density. Advances in stereolithography apparatus (SLA) three-dimensional (3D) printing and hard resins make it possible to fabricate such complex geometries precisely. The present study contrasts the mechanical performance of six geometries of TPMS under com-pressive loading with particular focus on how wall geometry and thickness affect it but at a fixed porosity of 75% and size of 70 × 70 × 70 mm^3. Among the structures, the peak compressive stress was the maximum in Gyroid (2.1 MPa), while Neovius demonstrated remarkably good performance (0.9 MPa) despite its low wall thickness. The objective is to analyze geometry-dependent performance trends in order to inform future structural design. These results imply that TPMS geometry can have a significant effect on mechanical response, regardless of wall thickness alone.

Keywords: TPMS structures; SLA 3D printing; mechanical properties

check for updates

Academic Editor: Francesco Arcadio

Published: 14 April 2025

Citation: Kavafaki, S.; Maliaris, G. Mechanical Characterization of Triply Periodic Minimal Surface Structures Fabricated via SLA 3D Printing Using Tough Resin: Influence of Geometry on Performance. *Eng. Proc.* **2025**, *87*, 46. https://doi.org/10.3390/engproc2025087046

Copyright: © 2025 by the authors. Licensee MDPI, Basel, Switzerland. This article is an open access article distributed under the terms and conditions of the Creative Commons Attribution (CC BY) license (https://creativecommons.org/licenses/by/4.0/).

1. Introduction

In engineering applications, high-energy characteristics are essential to minimize damage, often achieved through cellular structures inspired by randomly or periodically arranged microstructures found in nature. While not all cellular materials are lattice structures, lattice structures like Triply Periodic Minimal Surfaces (TPMS) can be considered a subset of cellular materials. In Additive Manufacturing (AM), utilizing lattice structures allows engineers to customize the properties and performance of a component independently of its material and overall shape. Choosing the appropriate lattice topology is essential to fully leverage the distinctive advantages of the lattice structure for the specific application [1].

Additive manufacturing enables the fabrication of materials with intricate cellular architecture, whereby progress in 3D printing techniques is increasing the possible configurations of voids and solids ad infinitum [2]. These architectures topologically represent three-dimensional spatial structures, which can also be considered as a porous material structure [3]. These structures are gaining increasing significance because their design and fabrication have a significant role in mechanical behavior. They offer increased surface area, pore network interconnectivity, decreased mass, and light weight over their bulk counterparts [4].

Triply periodic minimal surface (TPMS) structures represent an emerging area of study in material science and engineering due to their unique geometric properties and versatile applications [5]. TPMS structures are characterized by their periodic minimal surfaces, which minimize surface area for a given boundary, resulting in highly efficient material distributions [6]. TPMSs are composed of infinite, non-self-intersecting, periodic surface structures in three principal directions and are associated with the crystallographic space group symmetry [7].

Particularly, stereolithography (SLA) 3D printing has emerged as a transformative technology for fabricating complex geometries with high precision [8]. Among these geometries, triply periodic minimal surface (TPMS) structures have gained significant attention due to their unique combination of lightweight properties, high surface area, and excellent mechanical performance [9]. These features make TPMS structures ideal for a wide range of applications, including energy absorption, biomedical implants, and structural components in engineering.

While earlier studies have compared TPMS mechanical behavior based on porosity alone [10–13], none have addressed the wall thickness variation that arises from the geometric nature of different TPMS equations. This study bridges that gap by examining specifically how wall thickness variations—arising from the achievement of constant porosity—affect structural performance, providing a more detailed insight into TPMS mechanics beyond porosity. Moreover, the majority of the existing literature has focused on metallic [9,14–16] or thermoplastic polymeric structures [10,17–21], with limited data regarding SLA-printed resin-based TPMS lattices. The gap in the literature emphasizes the need to examine how different TPMS geometries mechanically behave when manufactured by stable SLA resins with similar porosity restrictions.

The scope is to describe the uniaxial compressive behavior of six geometries of TPMS—Gyroid, Primitive, Diamond, Lidinoid, Neovius, and SplitP—each of which was created in nTop software that allows explicit generation and control of implicit TPMSs. The geometries were 3D printed with SLA at a fixed porosity of 75%. The aim is to investigate how geometry variations influence mechanical performance and identify design trends that will be beneficial for future application of TPMS in structure and biomedical applications.

The mechanical behavior of TPMS structures is strongly influenced by their geometry, porosity, and material properties. While thicker walls generally enhance the strength and stiffness of a structure, the intricate interplay between geometry and mechanical behavior can lead to unexpected results. This study investigates the mechanical performance of six TPMS geometries—Gyroid, Primitive, Diamond, Lidinoid, Neovius, and SplitP—fabricated using SLA 3D printing.

2. Materials and Methods

2.1. Sample Preparation

The TPMS structures investigated in this study were designed and generated using nTop, a computational design software tailored for advanced lattice and geometric modeling. Six distinct TPMS geometries—Gyroid, Primitive, Diamond, Lidinoid, Neovius, and SplitP—were created using the software's lattice generation tools. Each structure was designed with consistent external dimensions of $70 \times 70 \times 70$ mm^3 and the uniform 75% porosity as being was calculated directly within nTop software, enabling a systematic evaluation of the influence of geometry on mechanical behavior. The wall thicknesses of the various TPMS structures are summarized in Table 1. As detailed in Table 1, the wall thickness varies significantly among the TPMS geometries, with Gyroid being the thickest and Neovius the thinnest.

Table 1. Dimensions and wall thicknesses of the TPMS structures studied.

TPMS Geometry	Wall Thickness (mm)
Neovius	0.31
Lidinoid	1.17
Primitive	1.31
SplitP	1.33
Diamond	1.94
Gyroid	2.32

Wall thickness varies because each TPMS geometry has a different mathematical surface function and curvature distribution, which affects how material must be distributed to achieve a target porosity. Their surfaces are defined by the equations [10] that are shown on Table 2.

Table 2. Mathematical equations to generate the TPMS structures.

Pattern Name	Pattern	Mathematical Expression *f(x,y,z)*=
Gyroid	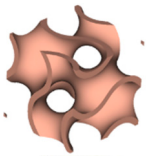	$sin(x) * cos(y) + sin(y) * cos(z) + sin(z) * cos(x)$
Primitive	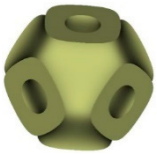	$cos(x) + cos(y) + cos(z)$
Diamond	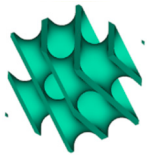	$sin(x) * sin(y) * sin(z) + sin(x) * cos(y) * cos(z) + cos(x) * sin(y) * cos(z) + cos(x) * cos(y) * sin(z)$
Lidinoid		$0.5 * [sin(2x) * cos(y) * sin(z) + sin(2y) * cos(z) * sin(x) + sin(2 * z) * cos(x) * sin(y) - cos(2x) * cos(2y) - cos(2y) * cos(2z) - cos(2z) * cos(2x) + 0.3]$
SplitP	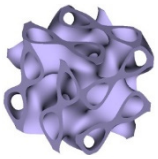	$1.1 * [sin(2x) * sin(z) * cos(y) + sin(2y) * sin(x) * cos(z) + sin(2z) * sin(y) * cos(x)) - 0.2 * (cos(2y) * cos(2y) + cos(2 * y) * cos(2z) + cos(2z) * cos(2x)) - 0.4 * (cos(2x) + cos(2y) + cos(2z)]$
Neovius' surface	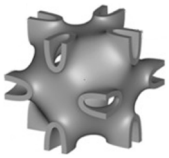	$3 * (cos(x) + cos(y) + cos(z)) + 4 * cos(x) * cos(y) * cos(z)$

When the porosity needs to held constant (75%) across different TPMS types, in the software the wall thickness is being adjusted individually to match the internal solid volume defined by the implicit surface function. This is a mathematical consequence of the TPMS equations.

The designed lattices were meshed with the usage of nTop in order to ensure high geometric accuracy and then exported as STL files. These STL files were processed for

fabrication using stereolithography (SLA) 3D printing technology. The resin that was used to print the structures was the tough engineering resin Siraya Tech Blu-Tough Resin. The printed specimens are depicted in Figure 1. According to the manufacturer's data, this resin exhibits the following properties: tensile strength of 44–48 MPa, Young's modulus of approximately 1700 MPa, and elongation at break of 25–30%.

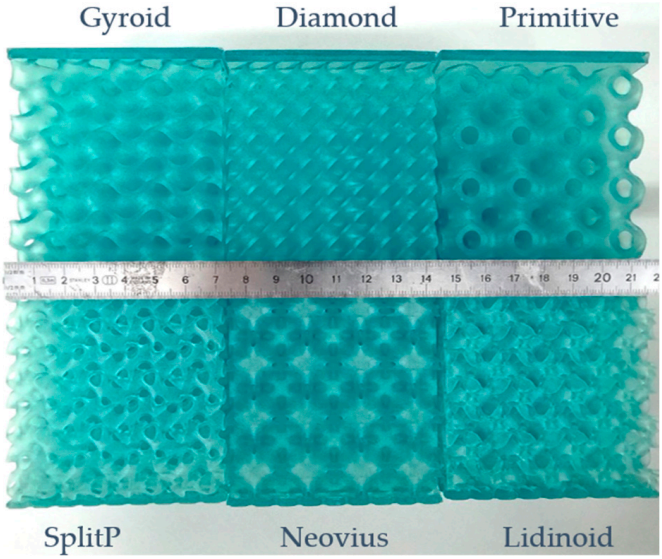

Figure 1. The six printed TPMS geometries.

After being printed, the samples were doused in isopropyl alcohol in order to remove any excess resin. To maintain consistency in mechanical performance and prevent the surface from becoming more brittle than the internal mass, the specimens were not UV cured. Lack of UV curing was determined to be an important factor in preserving uniform mechanical behavior throughout the entire structure, avoiding discrepancies between surface and internal material properties. Incomplete post-curing can cause over-hardening of outer surfaces while leaving the inner structure under-cured, leading to brittle outer layers and mechanical inconsistency [22].

2.2. Methodology

Compression tests were conducted in accordance with ASTM D695 Standard Test Method for Compressive Properties of Rigid Plastics [23] standards procedure for determining the compressive properties of rigid materials to evaluate the mechanical response of the TPMS structures. A universal testing machine (VTS model WDW-10) equipped with a 10 kN load cell force gauge was used to perform the tests, as shown in Figure 2. Each sample was subjected to uniaxial compression at a deformation rate of 2 mm/min [21] as shown in Figure 1.

Stress–strain curves were recorded during testing to assess the elastic and plastic deformation behaviors of the structures. For each of the six TPMS geometries, three replicate specimens (n = 3) were fabricated and tested under identical conditions to ensure statistical reliability. Particular care was taken in the elastic zone, where the response to stress was measured and compared with wall thickness and geometric measurements. Energy absorption (area under the curve) and structural failure modes were also tracked.

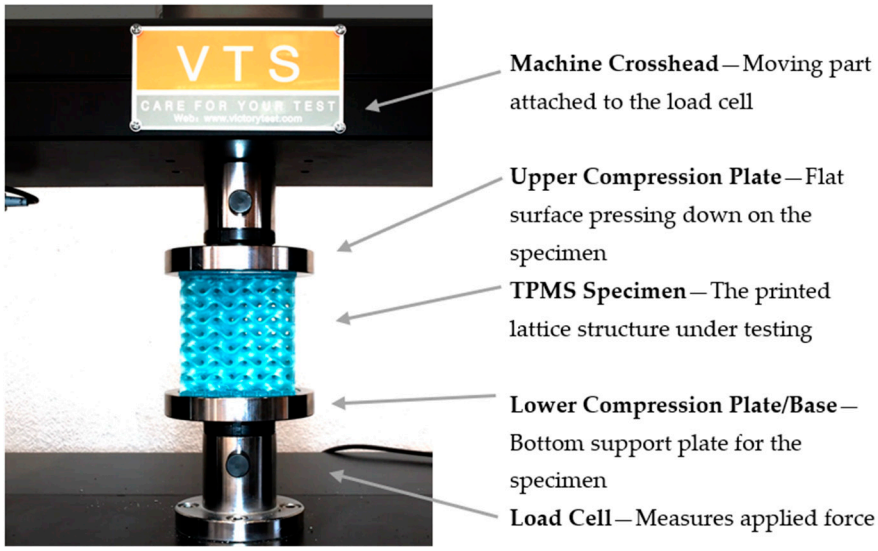

Figure 2. The compression testing apparatus on Gyroid TPMS geometry.

3. Results and Discussion

The mechanical response of the six TPMS lattice structures under uniaxial compression is illustrated in Figure 3, showing stress–strain curves up to 30% strain. All samples were fabricated with identical porosity (75%) and outer dimensions ($70 \times 70 \times 70$ mm^3), isolating the effect of geometry and wall thickness on mechanical performance. The six TPMS types, in descending order of wall thickness, are as follows: Gyroid, Diamond, SplitP, Primitive, Lidinoid, and Neovius. The curves are arranged by order of decreasing wall thickness, starting with the Gyroid structure (2.32 mm) and ending with the Neovius structure (0.31 mm). The results highlight significant differences in mechanical performance that are influenced by wall thickness, as well as geometry.

In this case, compression tests were conducted, as they reflect the mechanical loading requirements of typical TPMS applications like bone scaffolds, shock-absorbing protective layers, and light-weight structural components. Such application cases largely involve compressive loading conditions. While TPMS structures are indeed used in a broad variety of applications, several of them share in common the resisting deformation upon compressive loading, which justifies the experimental scope of this study.

The Gyroid structure, equipped with the thickest walls (2.32 mm), displayed the highest stress response throughout the elastic region, reaching a peak stress of approximately 2.1 MPa at 30% strain. Its inherently strong TPMS geometry, combined with its substantial wall thickness, enabled a superior load-bearing capacity and gradual stress increase, making it highly suitable for applications requiring high stiffness and mechanical strength. The Diamond structure, with a slightly thinner wall thickness (1.94 mm), displayed similarly high durability, achieving a peak stress of approximately 1.8 MPa. While its stress–strain curve closely resembles that of the Gyroid, the reduced wall thickness of the Diamond structure results in a slightly lower stiffness. Both geometries demonstrate efficient load distribution, highlighting their potential for applications that prioritize structural integrity under high loads. The SplitP structure, with a wall thickness of 1.33 mm, displayed a moderate stress response, reaching a peak stress of approximately 1.2 MPa, slightly outperforming the Primitive structure (1.31 mm), which peaked at 1.0 MPa. This behavior suggests that SplitP's geometry better balances structural stability and wall thickness. The Lidinoid structure, with walls 1.17 mm thick, demonstrated the lowest stress response among the tested geometries, peaking at approximately 0.8 MPa, indicating limited stiffness and suitability for lightweighting applications rather than load-bearing. Notably, the Neovius structure,

despite having the thinnest walls (0.31 mm), performed surprisingly well, achieving a peak stress of approximately 0.9 MPa. This result underscores the significant influence of geometry on stress absorption and load distribution, illustrating that a well-designed geometry can compensate for thinner walls in certain cases.

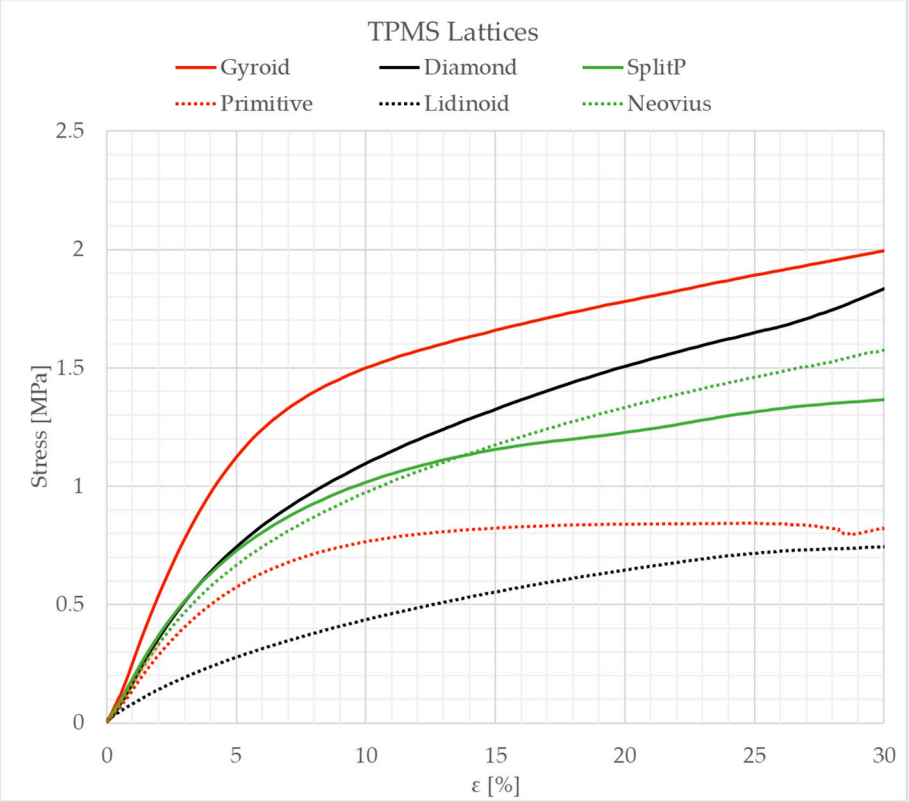

Figure 3. Stress–strain curves of TPMS structures under compression, ordered by decreasing wall thickness.

The stress–strain responses showed clear distinguishments in the mechanical behavior of the six TPMS structures. In the elastic zone, greater stress was observed in the following increasing order: Lidinoid, Primitive, Neovius, SplitP, Diamond, and Gyroid. While thicker walls generally resulted in higher stress, geometry had a significant influence on performance. Neovius, despite having the thinnest walls (0.31 mm), ranked fourth in stress, illustrating that wall thickness alone cannot fully predict mechanical behavior. Similarly, SplitP and Diamond exhibited nearly identical stress–strain curves, indicating comparable mechanical properties despite differences in wall thickness. Gyroid, with the thickest walls, displayed the highest stress in the elastic zone, aligning with the general trend of increased stress for thicker walls. These results highlight the complex interaction between geometry and wall thickness in determining the mechanical properties of TPMS structures.

Neovius, with the thinnest walls (0.31 mm), outperformed Primitive and Lidinoid, reaching ~1.4 MPa. This is counterintuitive, as thinner walls are typically linked to reduced mechanical strength. However, the Neovius surface includes tightly curved, interconnected regions that seem to enhance local stiffness and delay the onset of failure. This indicates that geometry can overcome wall thickness effects, at least when the surface topology promotes structural bracing and load redirection.

For every TPMS structure, the energy absorption and the Young's Modulus were calculated and summarized in Table 3, based on three tests on each structure.

Table 3. Mechanical behavior of TPMS structures.

Structure	Wall Thickness [mm]	Young's Modulus [MPa]	Standard Deviation [MPa]	Energy Absorption at 30% Strain [MPa]
Gyroid	2.32	25.44	0.049	0.453
Diamond	1.94	17.61	0.041	0.365
SplitP	1.33	18.78	0.022	0.310
Primitive	1.31	14.35	0.041	0.216
Lidinoid	1.17	7.65	0.039	0.152
Neovius	0.31	16.70	0.037	0.323

To assess the elasticity of each TPMS structure, Young's Modulus was calculated by calculating the slope of the test with median values, shown in Table 3, along with the standard deviation for each structure.

To assess each TPMS structure's energy absorption capacity, the area under the stress–strain curves up to 30% strain was calculated and summarized in Table 2. This area quantifies the energy absorbed per unit volume, an essential metric for evaluating impact resistance and damping properties.

The Gyroid structure absorbs the most energy, in line with its superior stiffness and stress resistance. Interestingly, Neovius ranks third, despite its minimal wall thickness. This again highlights the impact of geometrical efficiency: Neovius' network of interlinked, high-curvature surfaces appears to allow controlled deformation and delayed densification, improving its shock mitigation ability. The Gyroid and Diamond structures showed superior energy absorption, consistent with their higher stiffness and strength. Neovius, despite its minimal wall thickness, surpassed both Primitive and Lidinoid, demonstrating the geometrical efficiency in stress distribution and energy dissipation.

The experimental results highlight the potential for customizing mechanical properties through TPMS design. Structures like Gyroid and Diamond, which exhibit high stress resistance, are promising for applications requiring load-bearing capability and structural integrity. Conversely, Neovius and SplitP structures, which combine moderate strength with energy absorption, could be optimized for applications such as biomedical implants or impact-resistant materials.

This study indicates the significance of wall thickness variations due to the geometrical character of different TPMS geometries even at fixed porosity. The geometrical structure plays a large influence on stiffness and also on energy absorption, regardless of the material volume. The abnormal nature of the Neovius structure, which is equivalent to thicker-walled configurations in energy absorption and strength, also validates this observation. In addition, by using SLA-printed resin structures, new experimental evidence is introduced to a field that is largely dominated by metallic or thermoplastic lattices.

4. Conclusions

This study underscores the critical role of both wall thickness and geometry in shaping the mechanical behavior of triply periodic minimal surface (TPMS) structures. While a general trend was observed where thicker walls correlate with higher stress in the elastic zone, the exceptional performance of the Neovius structure challenges this notion, emphasizing that geometry can, in some cases, play a more dominant role than wall thickness. The intricate interplay between structural design and material properties highlights the versatility and adaptability of TPMS structures for tailoring mechanical performance to specific requirements.

By harnessing advanced TPMS designs and utilizing tough engineering resins, this work demonstrates the feasibility of producing lightweight yet robust components with

enhanced stress distribution and energy absorption capabilities. These findings have far-reaching implementations, particularly in engineering applications requiring high strength-to-weight ratios and in medical devices where optimized mechanical properties are critical. The insights gained from this study pave the way for the development of innovative, high-performance structures that leverage the synergies between material selection, wall thickness, and geometry to meet the demands of modern engineering and biomedical challenges.

The key contribution of this research is to demonstrate that, with constant porosity, TPMS surface geometry and wall thickness together control mechanical performance—a relationship that has not been widely quantified in resin-based SLA-printed lattices. The findings introduce new insight into how different forms of TPMS structures behave under compression and can guide future material selection and design optimization for engineering and biomedical applications.

Author Contributions: S.K. and G.M. contributed to the conceptualization of the research article. S.K. contributed to the Methodology of the present article by planning the experiments. The Validation of the experiments was carried out by S.K. and G.M. The Investigation was carried out by S.K., while Resources were provided by G.M. The Writing—Original Draft was prepared by S.K., while the Writing—Review and Editing was carried out by S.K. and G.M. All authors have read and agreed to the published version of the manuscript.

Funding: This research received no external funding.

Institutional Review Board Statement: Not applicable.

Informed Consent Statement: Informed consent was obtained from all subjects involved in the study.

Data Availability Statement: Data are contained within the article.

Conflicts of Interest: The authors declare no conflicts of interest.

References

1. Fisher, J.W.; Miller, S.W.; Bartolai, J.; Simpson, T.W.; Yukish, M.A. Catalog of triply periodic minimal surfaces, equation-based lattice structures, and their homogenized property data. *Data Brief* **2023**, *49*, 109311. [CrossRef] [PubMed]
2. Schaedler, T.A.; Carter, W.B. Architected Cellular Materials. *Annu. Rev. Mater. Res.* **2016**, *46*, 187–210. [CrossRef]
3. Guo, X.; Zheng, X.; Yang, Y.; Yang, X.; Yi, Y. Mechanical behavior of TPMS-based scaffolds: A comparison between minimal surfaces and their lattice structures. *SN Appl. Sci.* **2019**, *1*, 1145. [CrossRef]
4. Benedetti, M.; Plessis, A.D.; Ritchie, R.O.; Dallago, M.; Razavi, S.M.J.; Berto, F. Architected cellular materials: A review on their mechanical properties towards fatigue-tolerant design and fabrication. *Mater. Sci. Eng. R Rep.* **2021**, *144*, 100606. [CrossRef]
5. Gado, M.G.; Al-Ketan, O.; Aziz, M.; Al-Rub, R.A.; Ookawara, S. Triply Periodic Minimal Surface Structures: Design, Fabrication, 3D Printing Techniques, State-of-the-Art Studies, and Prospective Thermal Applications for Efficient Energy Utilization. *Energy Technol.* **2024**, *12*, 2301287. [CrossRef]
6. Pugliese, R.; Graziosi, S. Biomimetic scaffolds using triply periodic minimal surface-based porous structures for biomedical applications. *SLAS Technol.* **2023**, *28*, 165–182. [CrossRef]
7. Hyde, S.; Blum, Z.; Landh, T.; Lidin, S.; Ninham, B.W.; Andersson, S.; Larsson, K. *The Language of Shape: The Role of Curvature in Condensed Matter: Physics, Chemistry and Biology*; Elsevier: Amsterdam, The Netherlands, 1996.
8. Lodhi, S.K.; Gill, A.Y.; Hussain, I. 3D Printing Techniques: Transforming Manufacturing with Precision and Sustainability. *Int. J. Multidiscip. Sci. Arts* **2024**, *3*, 129–138. [CrossRef]
9. Jin, M.; Feng, Q.; Fan, X.; Luo, Z.; Tang, Q.; Song, J.; Ma, S.; Nie, Y.; Jin, P.; Zhao, M. Investigation on the mechanical properties of TPMS porous structures fabricated by laser powder bed fusion. *J. Manuf. Process* **2022**, *76*, 559–574. [CrossRef]
10. Miralbes, R.; Ranz, D.; Pascual, F.; Zouzias, D.; Maza, M. Characterization of additively manufactured triply periodic minimal surface structures under compressive loading. *Mech. Adv. Mater. Struct.* **2020**, *29*, 1841–1855. [CrossRef]
11. Karimipour-Fard, P.; Behravesh, A.H.; Jones-Taggart, H.; Pop-Iliev, R.; Rizvi, G. Effects of design, porosity and biodegradation on mechanical and morphological properties of additive-manufactured triply periodic minimal surface scaffolds. *J. Mech. Behav. Biomed. Mater.* **2020**, *112*, 104064. [CrossRef]

12. Sauermoser-Yri, M.; Veldurthi, N.; Wölfle, C.H.; Svartvatn, P.J.; Hoem, S.O.F.; Lid, M.J.; Bock, R.; Palko, J.W.; Torgersen, J. On the porosity-dependent permeability and conductivity of triply periodic minimal surface based porous media. *J. Mater. Res. Technol.* **2023**, *27*, 585–599. [CrossRef]
13. Song, K.; Wang, Z.; Lan, J.; Ma, S. Porous structure design and mechanical behavior analysis based on TPMS for customized root analogue implant. *J. Mech. Behav. Biomed. Mater.* **2021**, *115*, 104222. [CrossRef] [PubMed]
14. Qiu, N.; Wan, Y.; Shen, Y.; Fang, J. Experimental and numerical studies on mechanical properties of TPMS structures. *Int. J. Mech. Sci.* **2024**, *261*, 108657. [CrossRef]
15. Khanna, P.; Sood, S.; Mishra, P.; Bharadwaj, V.; Aggarwal, A.; Singh, S.J. Analysis of compression and energy absorption behaviour of SLM printed AlSi10Mg triply periodic minimal surface lattice structures. *Structures* **2024**, *64*, 106580. [CrossRef]
16. Sun, Q.; Sun, J.; Guo, K.; Wang, L. Compressive mechanical properties and energy absorption characteristics of SLM fabricated Ti6Al4V triply periodic minimal surface cellular structures. *Mech. Mater.* **2022**, *166*, 104241. [CrossRef]
17. Daynes, S. Isotropic cellular structure design strategies based on triply periodic minimal surfaces. *Addit. Manuf.* **2024**, *81*, 104010. [CrossRef]
18. Mishra, A.K.; Chavan, H.; Kumar, A. Effect of material variation on the uniaxial compression behavior of FDM manufactured polymeric TPMS lattice materials. *Mater. Today Proc.* **2021**, *46*, 7752–7759. [CrossRef]
19. Saleh, M.; Anwar, S.; Al-Ahmari, A.M.; Alfaify, A. Compression Performance and Failure Analysis of 3D-Printed Carbon Fiber/PLA Composite TPMS Lattice Structures. *Polymers* **2022**, *14*, 4595. [CrossRef]
20. Mishra, A.K.; Kumar, A. Compression Behavior of Triply Periodic Minimal Surface Polymer Lattice Structures. *Exp. Mech.* **2023**, *63*, 609–620. [CrossRef]
21. Cao, Y.; Lai, S.; Wu, W.; Sang, L.; Lin, Y.; Liu, T.; Liang, C.; Liu, W.; Zhao, Y. Design and mechanical evaluation of additively-manufactured graded TPMS lattices with biodegradable polymer composites. *J. Mater. Res. Technol.* **2023**, *23*, 2868–2880. [CrossRef]
22. Guttridge, C.; Shannon, A.; O'Sullivan, A.; O'Sullivan, K.J.; O'Sullivan, L.W. Effects of post-curing duration on the mechanical properties of complex 3D printed geometrical parts. *J. Mech. Behav. Biomed. Mater.* **2024**, *156*, 106585. [CrossRef] [PubMed]
23. *ASTM D695*; Standard Test Method for Compressive Properties of Rigid Plastics. American Society for Testing and Materials: West Conshohocken, PA, USA, 2023.

Disclaimer/Publisher's Note: The statements, opinions and data contained in all publications are solely those of the individual author(s) and contributor(s) and not of MDPI and/or the editor(s). MDPI and/or the editor(s) disclaim responsibility for any injury to people or property resulting from any ideas, methods, instructions or products referred to in the content.